# Contents

*This page intentionally left blank*

# Chapter 2

# Case study: the Lorenz '96 system

**TODO: Fix this paragraph** Historically, it has been common practice to develop and test new parametrisation techniques using simpler dynamical systems that share the key nonlinear, multi-scale and chaotic properties of the climate system. These analogue systems provide testbeds where the parametrisation problem is more tractable, avoiding the expense, effort and technicalities of fully-fledged climate models. The simplicity of these systems also helps to ensure the reproducibility of the results obtained. This section will review the progress that has been made using simple analogue systems and argue that, considering the outstanding issues identified in §§ 1.2 and 1.3, further research using these systems may yet be warranted. The relevant techniques for constructing and testing parametrisation schemes in simple model frameworks, and the remaining open questions, will be discussed in order to inform future research.

## 2.1 The Lorenz '96 system

The Lorenz '96 model (henceforth L96) was proposed by eminent meteorologist Edward N. Lorenz in a 1995 paper (Lorenz 1995) on the growth of errors in solutions of dynamical systems and the resulting limits of predictability for those systems. Lorenz proposed to mimic the multi-scale nature of the climate system by coupling two dynamical systems with different characteristic time scales. Following his notation, there is a discrete set of "slow" variables $\{X_k\}_{k=1}^K$, each of which has an associated discrete set of "fast" variables $\{Y_{j,k}\}_{j=1}^J$. The indices of the slow variables are periodic ($X_{K+1} = X_1$ and $X_0 = X_K$) and the sets of fast variables are arranged end-to-end so that $Y_{J+1,k} = Y_{1,k+1}$ and $Y_{0,k} = Y_{J,k-1}$. The intuition is that the variables represent samples of a field along a latitude circle, as shown in Figure 2.1 (a reproduction of Figure 1 by Russell et al. (2017)). The evolution of the system is governed by the ordinary differential equations

$$\frac{\mathrm{d}X_k}{\mathrm{d}t} = -X_{k-1}(X_{k-2} - X_{k+1}) - X_k + F - \frac{hc}{b}\sum_{j=1}^{J} Y_{j,k}, \tag{2.1a}$$

$$\frac{\mathrm{d}Y_{j,k}}{\mathrm{d}t} = -cbY_{j+1,k}(Y_{j+2,k} - Y_{j-1,k}) - cY_{j,k} + \frac{hc}{b}X_k. \tag{2.1b}$$

The constant $c \geq 1$ dictates the ratio of the time scale of the $Y$ variables to the time scale of the $X$ variables, $b$ the typical magnitude of $X$ relative to $Y$, $h$ the strength of the coupling between the two subsystems and $F$ the constant forcing applied to each $X$ variable.

As discussed in § 1.1.2, the objective is to find $P_k(X_1, \ldots, X_K) \approx -(hc/b)\sum_{j=1}^{J} Y_{j,k}$ such that the solution of the parametrised system

$$\frac{\mathrm{d}X_k}{\mathrm{d}t} = -X_{k-1}(X_{k-2} - X_{k+1}) - X_k + F + P_k(X_1, \ldots, X_K)$$
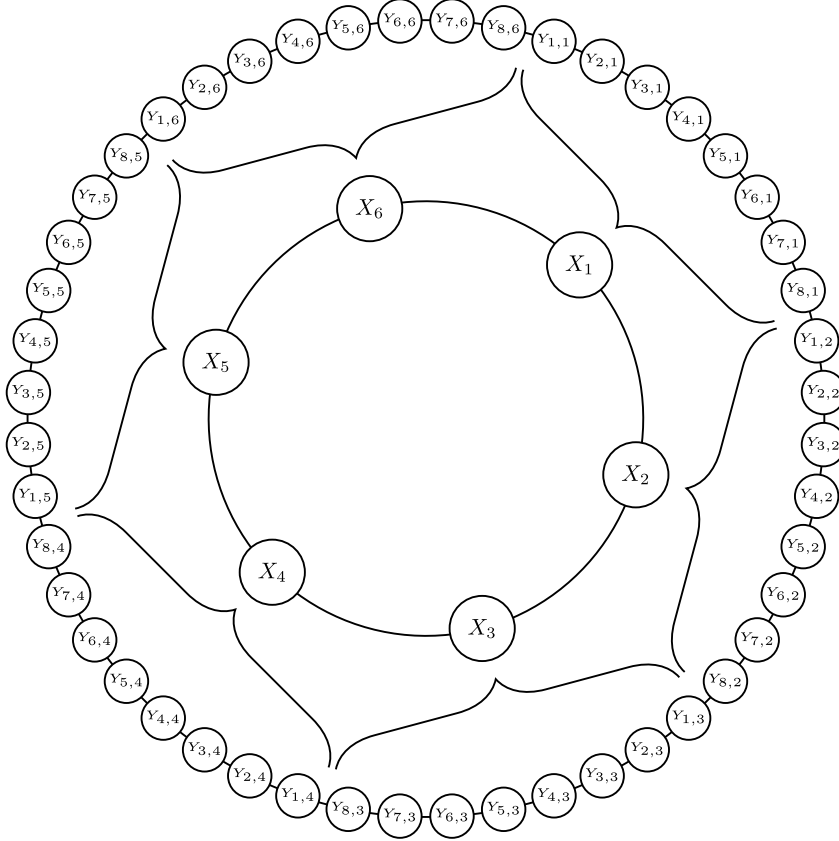
Figure 2.1: Illustration of the periodic arrangement of the L96 variables, with the slow variables $X_k$ arranged in a circle. Each slow variable is coupled to a neighbouring subset of the similarly arranged fast variables $Y_{j,k}$. Reproduced from Russell et al. (2017), Figure 1.

approximates as accurately as possible the true $X_k$ obtained by solving (2.1). The simple form of L96 allows one to generate a training dataset by numerically solving (2.1) and directly diagnosing the unresolved tendency of $X_k$ as

$$U_k(t) = \frac{X_k(t + \Delta t) - X_k(t)}{\Delta t} - [-X_{k-1}(X_{k-2} - X_{k+1}) - X_k]. \tag{2.2}$$

As we shall see, it is usually assumed that $P_k$ depends only on $X_k$ (i.e., the parametrisation is *local*) but may also depend on the value of $X_k$ at earlier times. The symmetry of (2.1) under shifts of the $k$ index implies that all the $X_k$ have the same long-term statistics, so it suffices to aggregate all the $U_k$ into a single training dataset and use the resulting parametrisation for all the $X_k$ rather than constructing a separate parametrisation for each variable.

## 2.2 Statistical models

Constructing a data-driven parametrisation scheme for L96 requires first choosing the structure of the scheme and then using the training dataset to find the optimal values of the associated free parameters. The simplest structure, popularised in an influential paper by Wilks (2005), consists of a polynomial regression of $U$ against $X$ as a deterministic base, modified by stochastic noise. Wilks' scatterplot of $U$ and $X$ and quartic polynomial least-squares regression, shown in Figure 2.2, confirm that such a structure is reasonable.
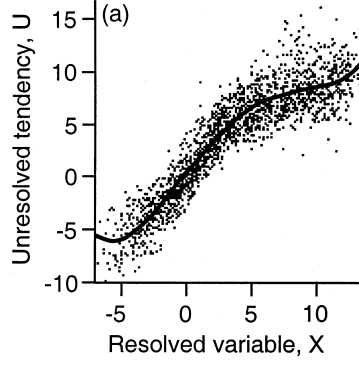
Figure 2.2:   Scatterplot of unresolved tendencies $U$ against large-scale variables $X$ in L96 (black dots), and corresponding quartic polynomial least-squares regression (black line). Data are for forcing $F = 18$. Reproduced from Figure 2a of Wilks (2005).

Denote the deterministic polynomial part of the parametrisation by $P_{\text{det}}(X)$. Wilks' proposal was to then model the residuals as an additive, mean-zero noise term $e(t)$, independent of $X$ and updated at each time step, so that

$$P(X) = P_{\text{det}}(X) + e(t). \tag{2.3}$$

Arnold, Moroz, and Palmer (2013) and later Christensen, Moroz, and Palmer (2015) considered the SPPT method (see § 1.3.1), where instead

$$P(X) = [1 + e(t)]P_{\text{det}}(X). \tag{2.4}$$

The most common form for $e(t)$ in both (2.3) and (2.4) is that of a *first-order autoregressive* or AR(1) model

$$e(t) = \phi e(t - \Delta t) + \sigma z \tag{2.5}$$

where $\phi \in [0, 1]$ and $\sigma \geq 0$ are constants and $z$ is drawn independently from the standard normal distribution at each time step. The AR(1) model introduces memory by having $e(t)$ relax from its value at the previous time step towards zero, while also adding independent random jumps with standard deviation $\sigma$. AR(1) noise is commonly also referred to as *red* noise. The two important special cases of an AR(1) model are $\phi = 0$, which reduces $e(t)$ to white noise without memory, and $\phi = \sigma = 0$, which results in a deterministic parametrisation $P(X) = P_{\text{det}}(X)$. The best estimates of $\phi$ and $\sigma$ are straightforwardly obtained by examining the autocorrelation and standard deviation of the residual time series $U(t) - P_{\text{det}}(X(t))$ in the training dataset (see Arnold, Moroz, and Palmer (2013) and Wilks (2011, Chapter 9) for details).

It must be noted that the additive and SPPT schemes (2.3) and (2.4) are inherently limited by their simple form. The additive scheme assumes that the variance of the unresolved tendency is independent of the value of $X$, and SPPT implies that the variance vanishes when $P_{\text{det}}(X) = 0$. Inspection of Figure 2.2 indicates that neither of these conditions is strictly satisfied. Arnold, Moroz, and Palmer (2013) therefore proposed two possible modifications of (2.3), with the standard deviation of $e(t)$ being a linear function of either $|X(t)|$ or $|P_{\text{det}}(X(t))|$.

Other studies have experimented with more complex statistical models for the unresolved tendencies. Chorin and Lu (2015) tested NARMAX (nonlinear autoregression moving average with exogenous inputs), a model which represents the tendency as a function of (i) the tendencies estimated at previous time steps (autoregression), (ii) the current and previous values of $X$ (nonlinear; exogenous data), (iii) independent Gaussian noise and (iv) the previous values of the Gaussian noise (moving average). The motivation for NARMAX is that it may be able to capture more complex relationships and memory effects by using more predictors and free parameters. Crommelin and Vanden-Eijnden (2008) and Kwasniok (2012) used Markov chain models, which approximate the continuous range of possible unresolved tendencies $U$ for a given $X$ by a discrete set of allowed states. The model transitions from state to state according

to a set of probabilities that depend on $X$ and are estimated from the training dataset. The latest studies have tested machine learning algorithms for L96, reflecting the increasing research interest in ML-based parametrisation schemes for GCMs (see § 1.3.2). Gagne II et al. (2020) used generative adversarial networks (GANs), which involve pairs of competing neural networks and have the advantage of being stochastic with no need for *ad hoc* perturbations. Bhouri and Gentine (2023) used deterministic but memory-based neural networks trained to directly optimise short-term forecast accuracy without requiring the calculation of the unresolved tendencies $U$ in the training dataset.

## 2.3    Evaluating parametrisation performance

After choosing and fitting a parametrisation scheme, the next step is to assess its performance. It is important to recognise that there are several contexts in which one might want a parametrisation to perform well. The first important distinction is between *offline* and *online* testing. Offline testing involves feeding large-scale states into the parametrisation scheme from a pre-computed test dataset that was not used for training (such as a new high-resolution simulation) and measuring the level of agreement between the tendencies predicted by the scheme and the true tendencies. Online testing, on the other hand, involves coupling the parametrisation scheme into the host model and comparing the output of the parametrised model to the corresponding "truth" solution (which might be the output of a high-resolution unparametrised model). Online performance can further be assessed for short-term ("weather") forecasts or long-term ("climate") predictions. The reliability of ensemble forecasts (see § 1.3.1) must also be determined. As we shall see, the extent to which good performance in more than one category is achievable is a topic of ongoing research.

### 2.3.1    Offline testing

Offline testing is rarely documented in the L96 literature because it is somewhat more straightforward than online testing. The aim is to ensure that the parametrisation scheme accurately captures the distribution of unresolved tendencies that exist in the true solution. Gagne II et al. (2020) achieved this by integrating the full system (2.1) to obtain a test dataset and estimating the time-aggregated probability density functions (PDFs) of the true unresolved tendencies (2.2) and the tendencies predicted by the parametrisation schemes. They then expressed the difference between these distributions as a scalar quantity using the Hellinger distance, defined for two PDFs $p$ and $q$ by

$$H(p, q) = \frac{1}{2} \int \mathrm{d}x \left( \sqrt{p(x)} - \sqrt{q(x)} \right)^2 . \tag{2.6}$$

### 2.3.2    Forecast performance

When evaluating online forecast accuracy for L96, studies are primarily concerned with the agreement between a "truth" (or verification) solution of (2.1) and the mean of an ensemble of independently realised, stochastically parametrised forecasts starting from the same or nearby initial conditions. This reflects standard practice in operational numerical weather prediction. A standard approach is to calculate the root mean square error (RMSE)

$$\mathrm{RMSE}(t) = \left( \left\langle \sum_k (X_k^{\mathrm{ens}}(t) - X_k^{\mathrm{ver}}(t))^2 \right\rangle \right)^{1/2}$$

between the ensemble mean forecast $X_k^{\mathrm{ens}}(t)$ and the verification $X_k^{\mathrm{ver}}(t)$, where the mean $\langle \cdot \rangle$ is taken over many forecast-verification pairs with a range of initial conditions (Crommelin and Vanden-Eijnden 2008; Gagne II et al. 2020).

An alternative for single-integration (non-ensemble) forecasts is to take the mean over time, from the initial time up to time $t$ (Bhouri and Gentine 2023). Another accuracy metric is the anomaly correlation (ANCR), which is the Pearson correlation coefficient

$$\text{ANCR}(t) = \left\langle \frac{\sum_k A_k^{\text{ens}}(t) A_k^{\text{ver}}(t)}{\left[ \left( \sum_k A_k^{\text{ens}}(t)^2 \right) \left( \sum_k A_k^{\text{ver}}(t)^2 \right) \right]^{1/2}} \right\rangle$$

between the forecast anomaly $A_k^{\text{ens}}(t) = X_k^{\text{ens}}(t) - \langle X_k^{\text{ver}}(t) \rangle_t$ and the verification anomaly $A_k^{\text{ver}}(t) = X_k^{\text{ver}}(t) - \langle X_k^{\text{ver}}(t) \rangle_t$, again averaged over forecast-verification pairs (Crommelin and Vanden-Eijnden 2008). Other studies (Kwasniok 2012; Arnold, Moroz, and Palmer 2013) have used more complex skill scores to assess forecast accuracy.

Recall from § 1.3.1 that an ensemble forecast is said to be reliable if the spread of the ensemble members is an accurate estimate of the uncertainty in the ensemble mean. In the context of L96, there are two ways to measure reliabilty. The first (Wilks 2005; Crommelin and Vanden-Eijnden 2008; Kwasniok 2012) is to sort the states $X_k$ of the ensemble members at the chosen lead time from largest to smallest (or vice versa), and find the rank that the truth state would occupy within the list. The ranks from many ensemble forecasts are aggregated and their distribution plotted on a *rank histogram*, which should ideally be uniform for a well-dispersed ensemble. A U-shaped rank histogram indicates underdispersion; that is, the truth too frequently lies at the extreme ends of or outside the ensemble. An inverted U shape indicates the opposite (overdispersion). Another method is to simply compare the ensemble standard deviation and the RMSE, which should be roughly equal for a reliable forecast (Arnold, Moroz, and Palmer 2013; Gagne II et al. 2020).

### 2.3.3 Climate prediction performance

There are several classes of metrics and methods available for assessing the accuracy of long-term climate predictions made by parametrised L96 models. The simplest is to compare the low-order moments (mean, variance) of the long-term distributions of $X$ between the parametrised and truth solutions. However, it is often the case for the relatively simple L96 model that parametrised models reproduce these moments quite accurately (Wilks 2005), motivating comparison of the entire PDFs—a more stringent test. In addition to visual comparison of the PDFs, one can use scalar measures such as the Hellinger distance (2.6) (Arnold, Moroz, and Palmer 2013; Gagne II et al. 2020) and the Kolmogorov-Smirnov statistic

$$D_n = \max_X |\Psi_{\text{true}}(X) - \Psi_{\text{model}}(X)|,$$

which is the maximum absolute difference between the cumulative distribution functions $\Psi$ of $X$ in the truth and parametrised models (Wilks 2005; Chorin and Lu 2015; Kwasniok 2012). As a diagnostic tool, it is also possible to compare the joint distributions of $X$ and the unresolved tendency $U$ between the truth and parametrised models (Gagne II et al. 2020).

Another approach is to study the correlation and spectral properties of $X$. In the time domain, one can compute the autocorrelation function $\langle X_k(t) X_k(t+\tau) \rangle_{t,k}$ or the cross-correlation $\langle X_k(t) X_{k+1}(t+\tau) \rangle_{t,k}$ between neighbouring variables and compare these to their truth counterparts (Crommelin and Vanden-Eijnden 2008; Kwasniok 2012; Chorin and Lu 2015; Gagne II et al. 2020). Gagne II et al. (2020) applied the continuous wavelet transform (CWT) to the $X(t)$ time series to measure the amount of power in the signal as a function of oscillation period. Similar analyses may be performed in "space" by computing the autocorrelation $\langle X_k(t) X_{k+n}(t) \rangle_{t,k}$ with respect to shifts in the $k$ index (Gagne II et al. 2020) or by taking a discrete Fourier transform of $X_k$ with respect to $k$ and deriving wavenumber statistics (Crommelin and Vanden-Eijnden 2008; Kwasniok 2012).

## 2.4   Lessons learnt from Lorenz '96

Now that the statistical models and analysis techniques for L96 parametrisation have been surveyed, I shall review the results of previous studies, focusing on key conclusions that have potential implications for more complex dynamical systems. The common objective in many studies has been to determine the value added by stochasticity and memory. The general consensus is that parametrisations with white noise outperform purely deterministic ones, and that adding memory via red noise or dependence on past large-scale states gives a further advantage over white noise (Wilks 2005; Arnold, Moroz, and Palmer 2013; Gagne II et al. 2020). The advantages of stochasticity and memory include improvements in the skill and reliability of ensemble forecasts and in the accuracy of climatological probability distributions. Arnold, Moroz, and Palmer (2013) additionally found that parametrisations with state-dependent noise have the potential to produce more skilful forecasts than those with state-independent additive noise. This was only observed under conditions of small time-scale separation between the resolved and unresolved variables (i.e., $c \sim 1$ in (2.1)); it appeared that simple additive noise was sufficient for larger scale separation. A representative illustration of the conclusions for short-term forecasting and climate prediction are respectively given by Figures 6 and 10 of Arnold, Moroz, and Palmer, which are reproduced here as Figures 2.3 and 2.4.
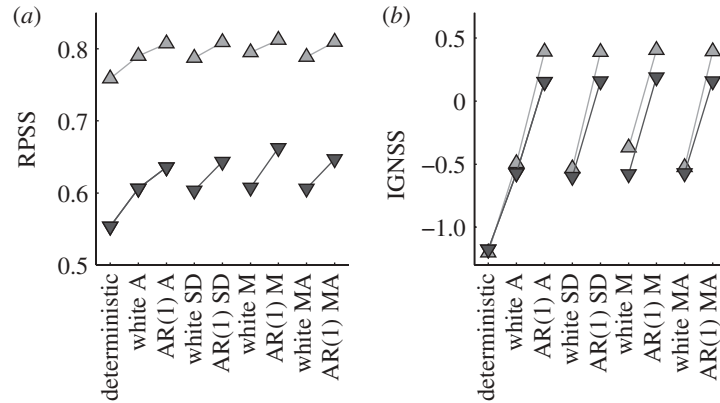


Figure 2.3:   Reproduction of Figure 6 by Arnold, Moroz, and Palmer (2013), showing a comparison of ensemble forecast skill for parametrisations with different types of noise. Skill is measured by the ranked probability skill score (RPSS; panel (a)) and ignorance skill score (IGNSS; panel (b)); higher values indicate better skill. The deterministic parametrisation is a cubic polynomial regression and added noise is either white or generated by an AR(1) process. Acronyms indicate the method used to introduce the noise; A = "additive", SD = "state-dependent" (noise standard deviation a linear function of $|X|$), M = "multiplicative" (SPPT) and MA = "multiplicative and additive" (noise standard deviation a linear function of $|P_{\text{det}}(X)|$). Upright light grey triangles indicate results obtained under conditions of larger time scale separation ($c = 10$ in (2.1)) and inverted dark grey triangles indicate smaller time scale separation ($c = 4$). It is clear that schemes with white noise outperform deterministic ones, and schemes with AR(1) noise outperform whose with white noise.
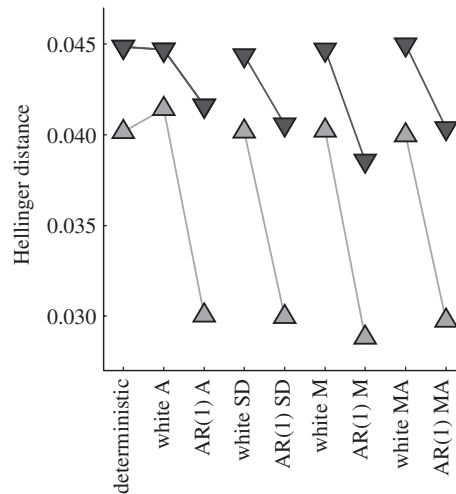
Figure 2.4:   Reproduction of Figure 10 by Arnold, Moroz, and Palmer (2013), comparing the accuracy with which parametrisations with different types of noise reproduce the true climatological PDFs of the resolved variables. Accuracy is measured by the Hellinger distance between the modelled and true PDFs; lower values indicate higher accuracy. The labels on the horizontal axis and the markers have the same meaning that they do in Figure 2.3. A clear improvement in accuracy is given by the schemes with AR(1) noise.

Some studies have obtained results that conflict with the aforementioned consensus. Firstly Arnold, Moroz, and Palmer (2013) found no appreciable difference in climatological PDF accuracy between their white noise and deterministic schemes; this is evident in Figure 2.4. Analogously, Christensen, Moroz, and Palmer (2015) similarly found no significant difference between white noise and deterministic schemes in terms of their ability to reproduce regime behaviour and predict the system's response to changes in the external forcing parameter $F$. Gagne II et al. (2020), who constructed parametrisations using generative adversarial networks, came to the unexpected conclusion that using temporally correlated red noise may degrade the accuracy of ensemble forecasts via an accumulation of noise-induced error and have little benefit over white noise for climate prediction accuracy.

Several authors have postulated general interpretations of these results that may be relevant to the parametrisation problem in dynamical systems beyond L96. Arnold, Moroz, and Palmer (2013) attributed the apparent superiority of memory-based parametrisations to a potential for subgrid-scale processes to influence the resolved state on scales much larger than the grid scale at which the host model is truncated; memory captures this spatial and temporal correlation or persistence. Christensen, Moroz, and Palmer (2015) agreed with this assessment on the basis of their results. They also argued that the persistence of correlated noise is necessary to drive regime transitions that would otherwise be underrepresented. Observing that stochastic parametrisation improved the prediction of responses to changes in forcing, they further argued that stochastic data-driven parametrisations are generally more likely to function well in changed climate conditions outside the range of their training datasets.

## 2.5   Open questions and the case for more complex dynamical systems

To conclude this section on data-driven parametrisation for L96, I will draw on the key messages and conclusions in the literature to motivate further research of the same kind in models of intermediate complexity.

Generally speaking, many parametrisation approaches of varying complexity have shown promise when

applied to L96; all the studies mentioned in § 2.2 were able to construct a scheme that reproduced the properties of interest without egregious errors. Indeed, some of the more recent and complex approaches have shown only marginal improvements over the original regression-based approach introduced by Wilks (2005). Gagne II et al. (2020) attributed this to the simplicity of L96, which only considers the evolution of a single field in one discrete spatial dimension. There is hope that applying the L96 methods to dynamical systems with more prognostic variables, spatial dimensions and degrees of freedom may reveal deficiencies that were inconsequential in L96 and thus give researchers more discriminative power in choosing approaches for application to full GCMs.

Several specific findings in L96 studies raise other questions that also motivate a change of focus to more complex dynamical systems. The first is the observation by Crommelin and Vanden-Eijnden (2008) that the advantage of their conditional Markov chain parametrisation over the regression-based approach was greatest under conditions of small time-scale separation and diminished with increasing scale separation. Arnold, Moroz, and Palmer (2013) drew a similar conclusion regarding the difference between stochastic and deterministic regression-based schemes. These findings are consistent with the expectation that the net effect of subgrid-scale processes should become increasingly unpredictable as resolution increases and the size of the sample of small-scale events decreases (see § 1.2.2). This is another piece of evidence that more realistic fluid models, which do not have such a clean separation between "resolved" and "unresolved" variables, will be more discriminating and allow the best approaches to show their full potential.

An open question of importance for real-world modelling concerns the extent to which parametrisation schemes that result in accurate weather forecasts tend can be expected to also produce accurate climate predictions (Christensen and Berner 2019). Another asks whether a scheme's offline performance is a good indicator of its online performance once coupled into a model. Gagne II et al. (2020) addressed these questions by testing a collection of GAN parametrisations with different predictors and types of noise (see Figure 2.5), with the results suggesting an affirmative answer for the former and a negative answer for the latter. The verification of these conclusions would be a worthwhile goal for further research using other dynamical systems. Other possible goals could be to more clearly assess the ability of data-driven parametrisation schemes to adapt to unseen climate conditions (Christensen, Moroz, and Palmer 2015) and to explore and exploit the potential for data-driven schemes to correct numerical errors in addition to modelling unresolved processes (Bhouri and Gentine 2023).
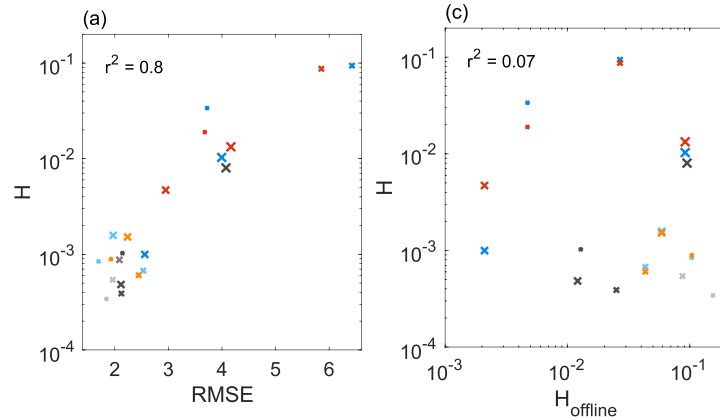


Figure 2.5:  Reproduction of Figures 11a and 11c by Gagne II et al. (2020). Panel (a) compares ensemble mean weather forecast accuracy (measured by RMSE) to climatological PDF accuracy (measured by the Hellinger distance $H$) for a collection of GAN parametrisations with different predictors and types of noise. Panel (c) performs a similar comparison with offline performance (measured by the Hellinger distance between the PDFs of the true and predicted tendencies) taking the place of RMSE.

## 2.6 Beyond Lorenz '96

The transition from L96 to more complex systems necessarily gives rise to several technicalities that must be addressed. The most pressing of these is the fact that increasing the number of degrees of freedom in the host model will greatly increase the number of predictors available for parametrisations to use. Models with more than one prognostic variable will also require separate parametrisations for each one. Without judicious simplifications, the problem of constructing a rigorous data-driven parametrisation will quickly become intractable. Crommelin and Vanden-Eijnden (2008) give an insightful discussion of this issue as it relates to Markov chain parametrisations.

Another complication is that the "spatial" dimension in L96 is discrete, while the dynamical systems being parametrised in weather and climate modelling (i.e., fluid flows) have continuous spatial dimensions. While it is well established that there is little benefit in using stochastic parametrisations with spatially correlated noise for L96, spatial correlation is expected to be a much more important consideration in spatially continuous systems (Arnold, Moroz, and Palmer 2013). One might also ask whether it will be beneficial to construct spatially nonlocal schemes where the tendency predicted at each point also depends on the values of the large-scale variables at neighbouring points (potentially capturing the gradients of these variables).

*This page intentionally left blank*

# Bibliography

Arnold, H. M., I. M. Moroz, and T. N. Palmer (2013). "Stochastic parametrizations and model uncertainty in the Lorenz '96 system". *Phil. Trans. R. Soc. A* **371**(1991). DOI: 10.1098/rsta.2011.0479.

Bhouri, M. A. and P. Gentine (2023). "Memory-based parameterization with differentiable solver: application to Lorenz '96". *Chaos* **33**(7). DOI: 10.1063/5.0131929.

Chorin, A. J. and F. Lu (2015). "Discrete approach to stochastic parametrization and dimension reduction in nonlinear dynamics". *PNAS* **112**(32). DOI: 10.1073/pnas.1512080112.

Christensen, H. M., I. M. Moroz, and T. N. Palmer (2015). "Simulating weather regimes: impact of stochastic and perturbed parameter schemes in a simple atmospheric model". *Clim. Dyn.* **44**(7). DOI: 10.1007/s00382-014-2239-9.

Christensen, H. M and J. Berner (2019). "From reliable weather forecasts to skilful climate response: a dynamical systems approach". *Q. J. R. Meteorolog. Soc.* **145**(720). DOI: 10.1002/qj.3476.

Crommelin, D. and E. Vanden-Eijnden (2008). "Subgrid-scale parameterization with conditional Markov chains". *J. Atmos. Sci.* **65**(8). DOI: 10.1175/2008JAS2566.1.

Gagne II, D. J., H. M. Christensen, A. C. Subramanian, and A. H. Monahan (2020). "Machine learning for stochastic parameterization: generative adversarial networks in the Lorenz '96 model". *J. Adv. Model. Earth Syst.* **12**(3). DOI: 10.1029/2019MS001896.

Kwasniok, F. (2012). "Data-based stochastic subgrid-scale parametrization: an approach using cluster-weighted modelling". *Phil. Trans. R. Soc. A* **370**(1962). DOI: doi:10.1098/rsta.2011.0384.

Lorenz, E. N. (1995). "Predictability: a problem partly solved". Seminar on Predictability (Shinfield Park, Reading). ECMWF. URL: https://www.ecmwf.int/en/elibrary/75462-predictability-problem-partly-solved.

Russell, F. P., P. D. Düben, X. Niu, W. Luk, and T. N. Palmer (2017). "Exploiting the chaotic behaviour of atmospheric models with reconfigurable architectures". *Comput. Phys. Commun.* **221**. DOI: 10.1016/j.cpc.2017.08.011.

Wilks, D. S. (2005). "Effects of stochastic parametrizations in the Lorenz '96 system". *Q. J. R. Meteorolog. Soc.* **131**(606). DOI: 10.1256/qj.04.03.

— (2011). *Statistical methods in the atmospheric sciences*. 3rd ed. International Geophysics. Amsterdam, Boston: Elsevier/Academic Press. ISBN: 0123850231.